# Methane Activation by $d^0$ and $d^2$ Imidos: Effects of d Orbital Occupation and Comparison of [2 + 2] and Oxidative Addition

Thomas R. Cundari[1]

*Department of Chemistry, Memphis State University, Memphis, Tennessee 38152*

*Received May 5, 1993*[⊗]

Methane activation by oxidative and [2 + 2] C—H addition to the $d^2$ imido $W(OH)_2(=NH)$ is investigated using effective core potential methods. The [2 + 2] C—H activation pathway is also compared with that for $d^0$ $Ti(OH)_2(=NH)$. Several points were deduced from the calculations. Although both the $d^0$ Ti— and $d^2$ W—imidos have a high positive charge on the metal, the former cannot coordinate weak Lewis bases such as methane. The [2 + 2] addition of the methane C—H bond across the metal—imido linkage is slightly exothermic for $Ti(OH)_2(=NH)$, $\Delta H_{rxn}$ = −11.7 kcal mol$^{-1}$, but endothermic for $W(OH)_2(=NH)$, $\Delta H_{rxn}$ = +23.4 kcal mol$^{-1}$. Oxidative addition is exothermic by 9.8 kcal mol$^{-1}$ for the $d^2$ W complex. The enthalpy of activation ($\Delta H^{\ddagger}_{act}$) for the [2 + 2] pathway is 55.2 kcal mol$^{-1}$ for $W(OH)_2(=NH)$ and 13.2 kcal mol$^{-1}$ for $Ti(OH)_2(=NH)$. The TS for $W(OH)_2(=NH) + CH_4 \rightarrow W(OH)_2(=NH)(H)(CH_3)$ is 22.3 kcal mol$^{-1}$ above that of reactants, much smaller than for the [2 + 2] pathway. The C—H bond length remains constant in length along the oxidative addition trajectory, until the TS is quite imminent. Similar behavior is observed for C—H along the [2 + 2] C—H activation trajectory. The changes in the C—H distance and M—H—C angle along the reaction coordinate are similar for [2 + 2] and oxidative addition in the portion of the reaction preceding the TS; energetic discrimination between the pathways does not occur since the reactions have proceeded well into the neighborhood of the respective transition states.

## Introduction

Selective activation of hydrocarbon C—H bonds is an important step in catalytic alkane functionalization.[2] Transition and lanthanide metal complexes which can effect C—H activation generally fall into two distinct groups. The first family is composed of high-valent ($d^0$ and $d^0f^n$) d- and f-block species, e.g. $Cp^*_2LuCH_3$ and $(N(H)Si\text{-}t\text{-}Bu_3)_2Zr{=}NSi\text{-}t\text{-}Bu_3$, which activate by [2 + 2] addition of C—H across a metal—ligand bond.[3] A second family activates by oxidative addition of C—H to an electron-rich, late transition metal complex.[4]

Complexes which are roughly intermediate between the extremes (possessing late but electrophilic transition metals, e.g. Pt(II) or Hg(II)) have recently garnered much interest for alkane functionalization.[5] These electrophilic systems are stable at ambient temperatures and in the presence of $O_2$ and $H_2O$.[5] The mechanism of C—H activation by electrophilic complexes is unclear, so that attempts to fine tune the metal and ligands to maximize activity and selectivity cannot proceed in a rational manner.[6] To build toward an understanding of electrophilic methane activators we have instituted two lines of research to complement previous[7] studies of methane activation by $d^0$ complexes. First, analysis of the reaction coordinates for typical high-valent[7] and low-valent[8] complexes makes it possible to compare at the most intrinsic level the electronic interactions which govern each. As a second strategy we have sought to minimize variables by researching complexes capable of effecting C—H activation by [2 + 2] and oxidative addition, i.e. $d^n$ complexes with $n \geq 2$. The present contribution describes our first attempt in this direction.

Activation of hydrocarbon C—H bonds by $d^0$ imidos has attracted experimental[3c,9–11] and computational[7] interest. Wolczanski et al. have characterized methane activation by bis(amido) Zr—imido,[3c] bis(imido) Ta—amido,[11a] and bis(alkoxy) Ti—imido[11b] transients. Bergman et al. have studied $Cp_2Zr{=}N\text{-}t\text{-}Bu$ and demonstrated its ability to C—H activate benzene[9a] and chlorinated derivates.[9b] Wigley et al.[11] observe C—H activation of terminal acetylenes by a $PMe_3$ adduct of $W(=NAr)_3$, Ar

⊗ Abstract published in *Advance ACS Abstracts*, September 1, 1993.

(1) e-mail: cundarit@memstvx1.memst.edu.

(2) *Activation and Functionalization of Alkanes*; Hill, C. L., Ed.; Wiley: New York, 1989.

(3) (a) Rothwell, I. P. In reference 2, p 151. (b) Watson, P. L. *J. Am. Chem. Soc.* **1983**, *105*, 6491. (c) Cummins, C. C.; Baxter, S. M.; Wolczanski, P. T. *J. Am. Chem. Soc.* **1988**, *110*, 8731.

(4) (a) Jones, W. D. In reference 2, p 111. (b) Crabtree, R. H. In reference 2, p 69. (c) Wasserman, E. P.; Moore, C. B.; Bergman, R. G. *Science* **1992**, *255*, 315.

(5) (a) Shilov, A. E. *Activation of Saturated Hydrocarbons*; Reidel: Boston, 1984. (b) Sen, A.; Lin, M.; Kao, L. C.; Hutson, A. C. *J. Am. Chem. Soc.* **1992**, *114*, 6385. (c) Labinger, J. A.; Herring, A. M.; Lyon, D. K.; Luinstra, G. A.; Bercaw, J. E., Horváth, I. T. *Organometallics*, in press. (d) Periana, R. A.; Taube, D. J.; Evitt, E. R.; Löffler, D. G.; Wentrcek, P. R.; Voss, G.; Masuda, T. *Science* **1993**, *259*, 340.

(6) As Sen notes, "more detailed mechanistic studies are required to fully understand the reactivity profile of the electrophilic metal species and how it can be influenced by the proper choice of the metal and the ligands." Sen, A. *Acc. Chem. Res.* **1988**, *21*, 421.

(7) (a) Cundari, T. R. *J. Am. Chem. Soc.* **1992**, *114*, 10557. (b) Cundari, T. R. *Organometallics* **1993**, *12*, 1998.

(8) Cundari, T. R. *J. Am. Chem. Soc.*, in press.

(9) (a) Walsh, P. J.; Hollander, F. J.; Bergman, R. G. *J. Am. Chem. Soc.* **1988**, *110*, 8729. (b) Bergman, R. G. Personal communication, Department of Chemistry, Berkeley.

(10) Chao, Y. W.; Rodgers, P. M.; Wigley, D. E.; Alexander, S. J.; Rheingold, A. L. *J. Am. Chem. Soc.* **1991**, *113*, 6326.

(11) (a) Schaller, C. P.; Wolczanski, P. T. *Inorg. Chem.* **1993**, *32*, 131. (b) Cummins, C. C.; Schaller, C. P.; Van Duyne, G. D.; Wolczanski, P. T.; Chan, A. W. E.; Hoffmann, R. *J. Am. Chem. Soc.* **1991**, *113*, 2985; personal communication.

0276-7333/93/2312-4971$04.00/0 

= 2,6-$C_6H_3$(*i*-Pr)$_2$. Recently, a series of $d^2$ imidos have been reported.[12-14] Schrock and co-workers have reported the crystal structure of Os(=NAr)$_3$,[12] while Wolczanski et al. have characterized W(=N-*t*-Bu)(O—Si-*t*-Bu$_3$)$_2$;[13] Schrock et al. observe Mo(=NAr)(OR$_f$), R$_f$ = fluorinated *tert*-butyl, as a side product in olefin metathesis.[14] Unlike $d^0$ imidos C—H activation by these $d^2$ imidos has not been observed although W(=N-*t*-Bu)(O—Si-*t*-Bu$_3$)$_2$ has recently been reported to oxidatively add $H_2$.[13]

As part of a continuing interest in the bonding[15] and reactivity[7] of imido complexes a computational investigation of C—H activation by a $d^2$ W—imido was undertaken. Although this and related $d^2$ imidos have not experimentally demonstrated C—H activating ability, through computation one can force the reactions to occur. By comparing [2 + 2] C—H activation for $d^0$ Ti(OH)$_2$(=NH) (a model of a putative methane activating transient[11b]) with $d^2$ W(OH)$_2$(=NH) we can evaluate the role of d orbital occupation in methane activation. In addition to the [2 + 2] C—H activation pathway, eq 1, the $d^2$ electron count for the W complex also makes oxidative addition, eq 2, a feasible pathway to C—H activation.

$$W(OH)_2(=NH) + CH_4 \rightarrow W(OH)_2(NH_2)(CH_3) \quad (1)$$

$$W(OH)_2(=NH) + CH_4 \rightarrow W(OH)_2(=NH)(H)(CH_3) \quad (2)$$

## Computational Methods

Our main approach to the challenges of the d- and f-block metals is the design, testing, and use of effective core potentials (ECPs).[16] Great savings in time, memory, and disk space are effected by replacing the core electrons, and the basis functions which describe them, with a small number of potentials. Relativistic effects are incorporated into ECP derivation. TM ECPs are generated from all-electron, Dirac-Fock calculations and thus include Darwin and mass velocity effects, while spin–orbit coupling is averaged out in potential generation.[16] From a chemical standpoint, ECP methods afford great leeway in the choice of interesting problems, particularly with respect to assessing the role of the central metal, since calculations on congeners within a triad are carried out with near equal facility. Thus, the search for improved catalyst and materials precursors can be carried out over a wider portion of the periodic table.

Calculations employ the computational chemistry program GAMESS.[17] GAMESS has recently been made to run in parallel. The iPSC/860 (128 nodes with 8Mb of memory per node) at Oak Ridge National Laboratories and the CM-5 at the University of Tennessee—Knoxville (32 nodes with 32 Mb per node) were used as parallel platforms. Calculations also employed the vectorized version of GAMESS on the Cray Y-MP/464 at the National Center for Supercomputer Applications and the serial version at Memphis State (RS-6000/350). Effective core potentials (ECPs) and valence basis sets are used for heavy atoms, and the -31G basis set is used for H. ECPs replace the innermost core orbitals for the TMs and all core orbitals for main-group (MG) elements. Thus, the ns, np, nd, $(n + 1)$s, and $(n + 1)$p are treated explicitly for the d-block; for the main group, ns and np are treated explicitly.[16] In the standard implementation, TM valence basis sets are quadruple- and triple-$\zeta$ for the sp and d shells, respectively, while main-group elements have a double-$\zeta$ valence basis.[16] Basis sets for heavy, main-group elements are augmented with a d polarization function.[18]

Geometries are optimized at the restricted Hartree–Fock (RHF) level for closed-shell singlets. Bond lengths and angles for ground state TM complexes are typically predicted to within several percent of experiment using the present scheme.[7,8,15] The effect of electron correlation on calculated geometries was assessed in previous studies of $H_2$ and methane activation/elimination.[7a,19] A multiconfiguration self-consistent field (MCSCF) study found small changes in stationary point geometries (including TSs) versus the much less computationally demanding RHF wavefunction; calculated intrinsic reaction coordinates at the RHF and MCSCF levels are nearly identical.[7a,19] These calculations point to the appropriateness of a single-determinant description of the potential energy surfaces.

Vibrational frequencies are calculated at stationary points to identify them as minima (zero imaginary frequencies) or transition states (one imaginary frequency). Plotting the imaginary frequencies is used to assess which TS connects which reactants and products. The intrinsic reaction coordinate (IRC) is followed using the Gonzalez–Schlegel algorithm.[20]

Although geometries are accurately predicted at the RHF level, energetics are expected to be poor if correlation is ignored. For species described well at the RHF level, the correlation contribution is a perturbation to the RHF energy and can be calculated using Moller–Plesset second-order perturbation theory (MP2).[21] An RHF geometry/MP2 energy scheme yielded good agreement[7a] with experimental data provided by Wolczanski[3c,11] for methane elimination from group IVB methyl complexes. A similar scheme has been shown to be appropriate in the study of oxidative addition.[8,21b,c]

## Results and Discussion

**1. Reactant Complexes.** The calculated structures for the model reactants, W(OH)$_2$(=NH) (**1a**) and Ti(OH)$_2$(=NH) (**1b**), are $C_{2v}$ minima. The calculated W—imido bond length of 1.71 Å compares with W—imido = 1.658(17)

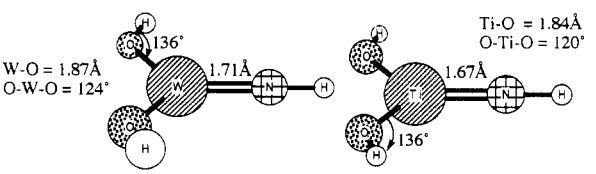


1a 1b

Å in (O—Si-*t*-Bu$_3$)$_2$W=N-*t*-Bu;[13] four-coordinate W(=C(H)Ph)(=NAr)(OCMe(CF$_3$)$_2$)$_2$ has W—imido = 1.708(1) Å.[22] Ti—imido bond lengths in structurally characterized examples range from 1.699(4) to 1.723(2) Å.[23] The W—O

(12) (a) Anhaus, J. T.; Kee, T. P.; Schofield, M. H.; Schrock, R. R. *Inorg. Chem.* **1991**, *30*, 3595. (b) Kee, T. P.; Anhaus, J. T.; Schrock, R. R.; Johnson, K. H.; Davis, W. M. *Inorg. Chem.* **1991**, *30*, 3595.

(13) Eppley, D. F.; Wolczanski, P. T.; Van Duyne, G. D. *Angew. Chem. Int. Ed. Engl.* **1991**, *30*, 584; personal communication.

(14) Robbins, J.; Bazan, G. C.; Murdzek, J. S.; O'Regan, M. M.; Schrock, R. R. *Organometallics* **1991**, *10*, 2902.

(15) Cundari, T. R. *J. Am. Chem. Soc.* **1992**, *114*, 7879.

(16) (a) Krauss, M.; Stevens, W. J.; Basch, H.; Jasien, P. G. *Can. J. Chem.* **1992**, *70*, 612. (b) Stevens, W. J.; Cundari, T. R. *J. Chem. Phys.* **1993**, *98*, 5555.

(17) (a) GAMESS: Schmidt, M. W.; Baldridge, K. K.; Boatz, J. A.; Jensen, J. H.; Koseki, S.; Gordon, M. S.; Nguyen, K. A.; Windus, T. L.; Elbert, S. T. *OCPE Bull.* **1990**, *10*, 52. (b) Schmidt, M. W.; Baldridge, K. K.; Boatz, J. A.; Jensen, J. H.; Koseki, S.; Matsunaga, N.; Gordon, M. S.; Nguyen, K. A.; Su, S.; Windus, T. L.; Elbert, S. T.; Montgomery, J.; Dupuis, M. *J. Comput. Chem.*, in press.

(18) Pople, J. A.; Hehre, W. J.; Radom, L.; Schleyer, P. v. R. *Ab-Initio Molecular Orbital Theory*; Wiley: New York, 1986.

(19) Cundari, T. R. *Int. J. Quantum Chem., Proc. 1992, Sanibel Symp.* **1992**, *26*, 793.

(20) Gonzalez, C.; Schlegel, H. B. *J. Chem. Phys.* **1989**, *90*, 2154.

(21) (a) Moller, C.; Plesset, M. S. *Phys. Rev.* **1934**, *46*, 618. (b) Koga, N.; Morokuma, K. *J. Phys. Chem.* **1990**, *94*, 5454. (c) Abu-Hasanayn, F.; Krogh-Jespersen, K.; Goldman, A. S. *Inorg. Chem.* **1993**, *32*, 495.

(22) Schrock, R. R.; DePue, R. T.; Feldman, J.; Schaverian, C. J.; Dewan, J. C.; Liu, A. H. *J. Am. Chem. Soc.* **1988**, *110*, 1423.

(23) (a) Hill, J. E.; Profilet, R. D.; Fanwick, P. E.; Rothwell, I. P. *Angew. Chem., Int. Ed. Engl.* **1990**, *29*, 664. (b) Roesky, H. W.; Voelker, H.; Witt, M.; Noltemeyer, M. *Angew. Chem., Int. Ed. Engl.* **1989**, *29*, 669. Roesky, H. W.; Raubold, T.; Witt, M.; Bohra, R.; Noltemeyer, M. *Angew. Chem., Int. Ed. Engl.* **1989**, *29*, 669. (c) Duchateau, R.; Williams, A. J.; Gambarotta, S.; Chaing, M. Y. *Inorg. Chem.* **1991**, *30*, 4863.

bond lengths are 1.87 Å in **1a**, 1.826(16) Å in $(OSi')_2W{=}N$-*t*-Bu,[13] and 1.903(16) and 1.904(14) Å in W(=C(H)-Ph)(=NAr)$(OCMe(CF_3)_2)_2$.[22] The Ti—O bond lengths of 1.84 Å are slightly longer than the values of 1.752(6) Å for $(Me)_2$(tritox)Ti($\mu$-OMe)$_2$Ti(tritox)$(Me)_2$ (tritox = OC-*t*-$Bu_3$) and 1.798 Å in Ti[O-2,6-$C_6H_3$(*t*-$Bu)_2$]$_3$I.[24] Calculated O—W—O and N=W—O angles in **1** are 124 and 118°, respectively; the experimental values are O—W—O = 127.4(6)° and N=W—O = 115.7(8) and 116.8(8)° in (O—Si-*t*-$Bu_3)_2$W=N-*t*-Bu.[13]

Despite the formal $d^2$ configuration of W in **1a**, the metal—imido linkage is still heavily polarized in a $M^{\delta+}{=}N^{\delta-}$ fashion. A Mulliken population analysis yields atomic charges of +1.54 (W), −0.81 (N), and −0.92 (O); for $Ti(OH)_2$(=NH) $q$(Ti) = +1.36, $q$(N) = −0.67, and $q$(O) = −0.86. The degree of metal—ligand polarization has been suggested as an important determinant of activating ability for high-valent C—H activators.[3c,25] The population analysis suggests that the metal is more positively charged in the $d^2$ complex and that the W—imido linkage is more polarized than the Ti—imido bond.[26] The molecular electrostatic potential maps for **1a** and **1b** are shown in Figure 1 for the plane perpendicular to the molecular plane and containing the metal—imido bond. Dotted lines show favorable sites for electrophilic attack while potential sites for nucleophilic attack are denoted by solid contours, Figure 1. Inspection of Figure 1 shows similar features for Ti and $W(OH)_2$(=NH): the imido N has appreciable nucleophilic character in both complexes with the metal having somewhat more electrophilic character in the $d^0$ complex. At first glance the $d^2$ W—imido seems well suited to activate methane in a [2 + 2] fashion.

Although calculated metal atomic charges on the $d^0$ Ti and $d^2$ W complexes are comparable, the former is expected to be a better Lewis acid. Experimentally, $W(OSi')_2$(=N-*t*-Bu) will not bind simple $\sigma$-donors like THF and can be isolated as a base-free complex,[13] while $d^0$ Ti—imidos are difficult to separate from donor ligands;[23] $Ti(OAr)_2$(=NPh) coordinates two bulky py′ (py′ = 4-pyrrolidinopyridine) ligands despite the bulky 2,6-diisopropylphenoxide ligands and the small covalent radius of Ti.[23a] The $W(OH)_2$(=NH) model can form a strongly bound complex[27] with ethylene (binding enthalpy = −43.2 kcal mol$^{-1}$), as experiment[13] indicates, but it is not a strong enough Lewis acid to bind methane. As part of a study of methane adduct formation by imido complexes it was noted that substrate–complex interaction was repulsive for $W(OH)_2$(=NH) but that binding methane to $d^0$ imidos such as $Ti(OH)_2$(=NH) and $W(=NH)_3$ was exothermic by −6.6 and −15.6 kcal mol$^{-1}$, respectively.[7b] The origin of the repulsive interaction is the metal-based, highest occupied molecular orbital (HOMO) in $d^2$ $W(OH)_2$(=NH); a similar orbital is the LUMO in $d^0$ $Ti(OH)_2$(=NH). Previous studies suggest that the reaction coordinate in the vicinity of the methane adduct is dominated by metal-to-substrate donation and that adduct formation is crucial in getting the reactants into the TS region.[8] The inability to form an adduct might be expected to inhibit the methane activating ability of electrophilic, but not $d^0$, complexes.

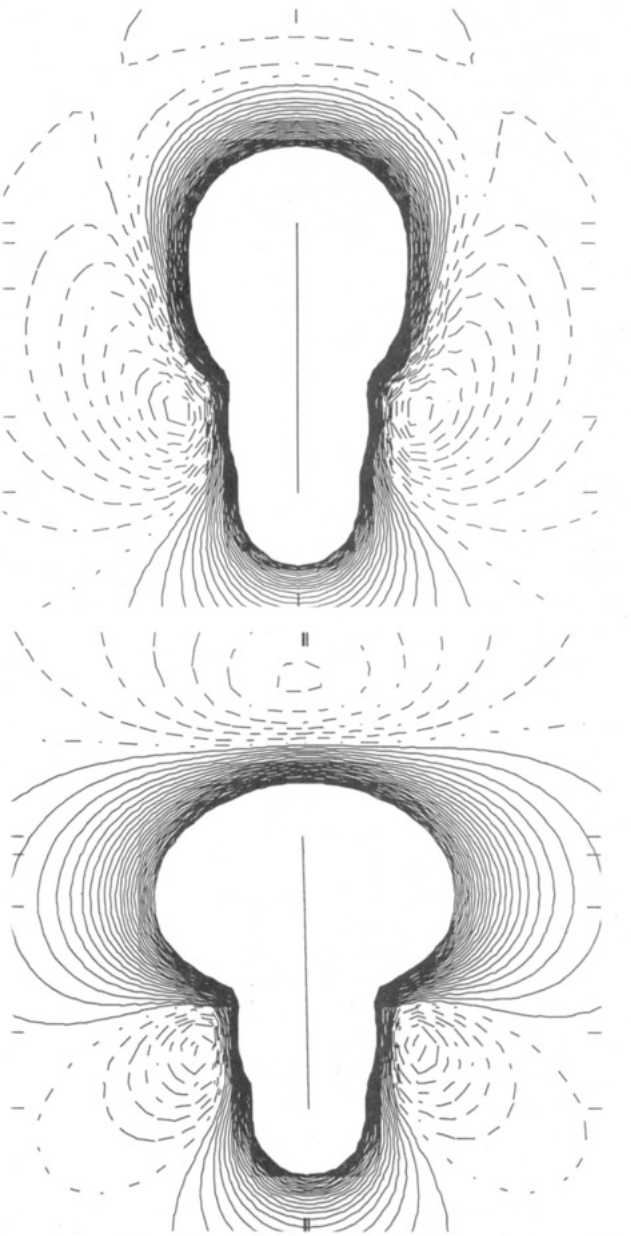

**Figure 1.** (a, Top) plot of the molecular electrostatic potential for $W(OH)_2$(=NH) in the plane perpendicular to the molecular plane, which contains the metal—imido bond. (b, Bottom) plot of the molecular electrostatic potential for $Ti(OH)_2$(=NH) in the plane perpendicular to the molecular plane, which contains the metal—imido bond.

**2. [2 + 2] Products.** The product of [2 + 2] C—H activation is four-coordinate $M(OH)_2(NH_2)(Me)$, **2a** (M = W) and **2b** (M = Ti). The geometry of **2a** is a distorted tetrahedron with a large O—W—O angle (145°) and very small O—W—C angles (95°). The N—W—O and

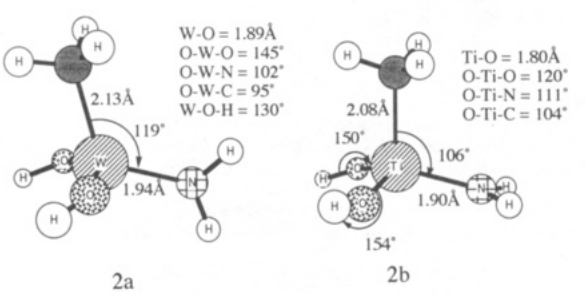


2a 2b

(24) Lubben, T. V.; Wolczanski, P. T. *J. Am. Chem. Soc.* **1987**, *109*, 424.

(25) (a) Fendrick, C. M.; Marks, T. J. *J. Am. Chem. Soc.* **1984**, *106*, 2214. (b) Thompson, M. E.; Baxter, S. M.; Bulls, A. R.; Burger, B.; Nolan, M. C.; Santarsiero, B. D.; Schaefer, W. P.; Bercaw, J. E. *J. Am. Chem. Soc.* **1987**, *109*, 203.

(26) As with any partitioning of the total electron density there is a degree of arbitrariness in the Mulliken population, although it is reasonable to expect trends for related complexes to be satisfactory.

(27) The calculated charge on the ethylene adduct of $W(OH)_2$(=NH) is very positive (+0.5), suggesting that the imido can act as a credible Lewis acid if the substrate is basic enough.

C—W—N angles are 102 and 119°, respectively. Bond angles about Ti in $Ti(OH)_2(NH_2)(CH_3)$ are closer to tetrahedral. Various $d^2$, four-coordinate third-row transition metal complexes $(Os(O)_2(mesityl)_2$,[28] $W(=NAr)_2(PMe_2Ph)(\eta^2\text{-}OCR_2)$,[29] and $Re(=NAr)_2(CH_2CMe_3)(2\text{-butyne})$[30] have recently been characterized; all exhibit diamagnetic ground states, while X-ray and NMR evidence support pseudotetrahedral geometries.[28-30] Diamagnetic, $d^2$ $Mo^{IV}$ $(NMe_2)_4$ has been structurally characterized; N—Mo—N bond angles range from 108.1(2) to 112.5(2)°.[31]

The W—O bond lengths in the [2 + 2] product are 1.89 Å, slightly longer (by 0.02 Å) than those in $W(OH)_2(=NH)$. On the other hand, the Ti—O bond lengths in **2b** are slightly shorter (by 0.04 Å) than those in **1b**. In both cases, calculated values remain in good accord with experimental values quoted above. The W—C bond lengths of 2.096(5) Å in $W(CH_2CMe_3)_2(\equiv CSiMe_3)$[32] are in excellent agreement with the calculated W—C bond length of 2.13 Å in **2a**. The mean W—C bond length in $W(CH_2CMe_3)_3(NEt_2)(O)$[33] is 2.19 Å. The Ti—C bond length of 2.08 Å in **2b** compares with Ti—C = 2.042(9) Å ($Cl_3TiMe$[34a]), 2.122(2) Å ($TiCl_3(dmpe)(Me)$[34b]), and 2.063(10) Å ($(Me)_2(tritox)Ti(\mu\text{-}OMe)_2Ti(tritox)(Me)_2$[24]). As expected, the W—N bond elongates considerably from 1.71 Å in **1a** to 1.94 Å in **2a**, a lengthening of 13%. The W—N bond length in $W(CH_2CMe_3)_3(NEt_2)(O)$[33] is 1.881(5) Å, while those in $(Me_2N)_3W{\equiv}W(NMe_2)_3$ and $Cl(NEt_2)_2W{\equiv}W(NEt_2)_2Cl$ are 1.98 and 1.94 Å, respectively.[35]

The enthalpy for reaction 3 (M = Ti, W) can be estimated from pertinent bond energies, eqs 4 and 5, where we assume the difference in the metal—amido and metal—imido bond

$$(OH)_2M{=}NH + CH_4 \rightarrow (OH)_2M(NH_2)(CH_3) \quad (3)$$

$$\Delta H_{rxn}([2+2]) \approx BDE_{M=N} + BDE_{H_3C-H} - BDE_{HN-H} - BDE_{MC} - BDE_{M-N} \quad (4)$$

$$\Delta H_{rxn}([2+2]) \approx \Pi_{MN} + 13 - BDE_{MC} \quad (5)$$

dissociation energies to be the MN $\pi$-bond energy ($\Pi_{MN}$) and the second term on the right is a constant (13 kcal $mol^{-1} \approx BDE_{H_3C-H} - BDE_{HN-H}$).[36a] Reaction 3 is slightly exothermic for M = Ti, $\Delta H_{rxn}$ = −11.7 kcal $mol^{-1}$, but decidedly endothermic for M = W, $\Delta H_{rxn}$ = +23.4, Chart I. Equation 5 suggests that calculated differences for Ti and W can be attributed to a weaker W—C bond (versus Ti—C) and/or a stronger WN $\pi$-bond (versus TiN). Of these possibilities the former is supported by the mean metal—methyl bond dissociation enthalpies for $Cp_2M\text{-}Me_2$: 68 kcal $mol^{-1}$ (M = Ti[36b]) and 53 kcal $mol^{-1}$ (M = W[36b]). The paucity of data for metal—ligand $\pi$-bond energies does not allow us to evaluate the latter assertion or the quantitative nature of the computational scheme. However, the calculated reaction enthalpies for eq 3 concur with the experimentally observed reactivity differences between the $d^0$ Ti— and $d^2$ W—imidos and suggest that the origin of this difference may be thermodynamic.[11b,13]

**3. [2 + 2] Transition State.** An initial search for [2 + 2] C—H activation transition states (TS) was carried out in $C_s$ symmetry, **3**. In **3a** and **3b** the $C_s$ plane contains the C—H atom being activated and the metal—imido bond

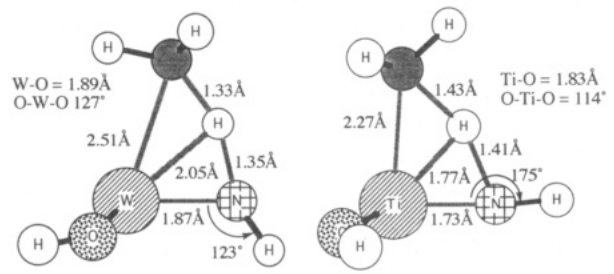


3a 3b

doing the activation. Stationary point **3a** possesses three imaginary frequencies, while the Ti analogue is a true TS at a related $C_s$ geometry, **3b**. The two high energy imaginary frequencies (2073i and 222i $cm^{-1}$) in **3a** correspond to C—H bond breaking/making and methyl group rotation, respectively. The smallest imaginary frequency (80i $cm^{-1}$) corresponds to twisting the $WO_2$ plane relative to that defined by the atoms (W, N, C, H) comprising the [2 + 2] active site.

Distortion of **3a** along the two low energy imaginary modes leads to **4** (viewed parallel to the W—N—C plane on the left and perpendicular to the W—N—C plane on the right) which is 33 kcal $mol^{-1}$ lower in energy at the

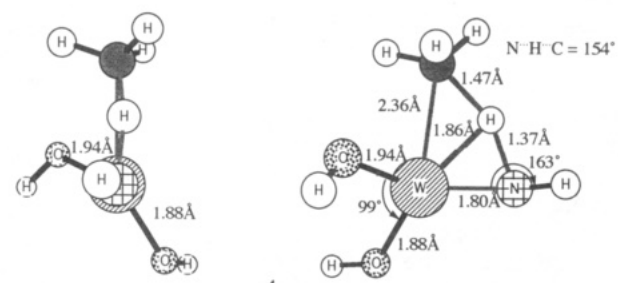


4

RHF level. Structure **4** is a true transition state (imaginary frequency = 1878i $cm^{-1}$), with the main motion in the TS corresponding to C—H bond breaking/making. Note the distortion of the $WO_2$ plane relative to the WNHC plane in **4**, as the 80i-$cm^{-1}$ mode indicated in **3a** was favorable.

The WN bond length in TS **4** is 1.80 Å, thus closer in length to the imido reactant than the amido product; a similar situation holds for the Ti case (**3b**). The angle between the metal—nitrogen bond and the exocyclic N—H bond (**3b** and **4**) is close to linear for Ti and W. The metric data point to an "early" TS for [2 + 2] C—H activation and thus a "late" TS for the reverse, methane elimination. Wolczanski et al.[3c] have deduced a late transition state for methane elimination from $d^0$ group IVB methyl(amido) complexes on the basis of activation parameters (large

(28) Stavropoulos, P.; Edwards, D. G.; Behling, T.; Wilkinson, G.; Motevalli, M.; Hursthouse, M. B. *J. Chem. Soc., Dalton Trans.* **1987**, 169.
(29) Schrock, R. R.; Williams, D. S.; Schofield, M. H.; Anhaus, J. T. *J. Am. Chem. Soc.* **1990**, *112*, 6728.
(30) Weinstock, I. A.; Schrock, R. R.; Williams, D. S.; Crowe, W. E. *Organometallics* **1991**, *10*, 1.
(31) Chisholm, M. H.; Cotton, F. A.; Extine, M. W. *Inorg. Chem.* **1978**, *17*, 1329.
(32) Caulton, K. G.; Chisholm, M. H.; Streib, W. E.; Xue, Z. *J. Am. Chem. Soc.* **1991**, *113*, 6082.
(33) Le Ny, J. P.; Youinou, M. T.; Osborn, J. A. *Organometallics* **1992**, *11*, 2413.
(34) (a) Berry, A. D.; Dawoodi, Z.; Derome, A. E.; Dickinson, J. M.; Downs, A. J.; Green, J. C.; Green, M. L. H.; Hare, P. M.; Payne, M. P.; Rankin, D. W. H.; Rohbertson, H. E. *J. Chem. Soc., Chem. Commun.* **1986**, 520. (b) Dawoodi, Z.; Green, M. L. H.; Mtetwa, V. S. B.; Prout, K.; Schultz, A. J.; Williams, J. M.; Koetzle, T. F. *J. Chem. Soc., Dalton Trans.* **1986**, 1629.
(35) Lappert, M. F.; Power, P. P.; Sangerand, A. R.; Srivasta, R. C. *Metal and Metalloid Amides*; Ellis Horwood: Chichester, U.K., **1980**; p 486.
(36) (a) *CRC Handbook*, 64th ed.; Weast, R. C., Ed.; CRC Press: Boca Raton, FL, 1983; p F-187. (b) Dias, A. R.; Salema, M. S.; Simoes, J. A. M. *J. Organomet. Chem.* **1988**, *346*, C4. Simoes, J. A. M.; Beauchamp, J. L. *Chem. Rev.* **1990**, *90*, 629.

$\Delta H^{\ddagger}_{elim}$ and large negative $\Delta S^{\ddagger}_{elim}$). As with previous [2 + 2] C—H activation transition states,[7a,37] there is a large angle about the H being transferred, as one would expect from the high kinetic isotope effects which have been measured for $d^0$ C—H activation systems.[3a] The short metal–transannular hydrogen distance (1.86 Å) is by now a familiar feature of the [2 + 2] TS;[7a,37] in the current example (**4**) the W—H distance is only 3% larger than that calculated for $O_h$ $WH_6$ (1.80 Å).[38]

The difference in calculated $\Delta H_{rxn}$ for [2 + 2] C—H activation by the $d^0$ Ti— and $d^2$ W—imidos is reflected in the activation barriers. The enthalpy of activation for C—H scission ($\Delta H^{\ddagger}_{act}$) is 55.2 kcal mol$^{-1}$ (versus separated reactants) for W(OH)$_2$(=NH). For the Ti analogue, $\Delta H^{\ddagger}_{act}$ = 19.8 kcal mol$^{-1}$ (versus the methane adduct) and 13.2 kcal mol$^{-1}$ (versus separated reactants), Chart I. The Ti values are in agreement with the only measured $\Delta H^{\ddagger}_{act}$ for C—H activation by a $d^0$ multiply bonded complex.[3a] Intramolecular C—H activation by the Ta=C bond in Ta(O-2,6-(*t*-Bu)$_2$-4-X-phenyl)$_2$(=CH$_2$)(CH$_3$) has $\Delta H^{\ddagger}_{act}$ = 14.3 ± 1.0 kcal mol$^{-1}$ (X = H) and 15.4 ± 1.0 kcal mol$^{-1}$ (X = OMe).[3a] The calculated enthalpy for methane elimination of W(OH)$_2$(NH$_2$)(CH$_3$) is 31.8 kcal mol$^{-1}$. The calculated value of $\Delta H^{\ddagger}_{elim}$ for Ti(OH)$_2$(NH$_2$)(CH$_3$) is 24.6 kcal mol$^{-1}$; using the calculated entropy of activation ($\Delta S^{\ddagger}_{elim}$ = −8.7 eu at $T$ = 298.15 K) yields a calculated $\Delta G^{\ddagger}_{elim}$ of 28.2 kcal mol$^{-1}$. Wolczanski et al.[11b] have measured $\Delta G^{\ddagger}_{elim}$ = 23 kcal mol$^{-1}$. The calculated $\Delta H^{\ddagger}_{elim}$ are in good accord with experimental data (as found previously in studies of methane activation by group IVB imidos[7a]) and support the notion that the main energetic contribution to the methane elimination barrier involves the bond making/breaking associated with the M(C)—N(H) → M=N + C—H reaction.

**4. Oxidative Addition Product.** Oxidative addition to a Ti(IV) complex would result in a physically unreasonable Ti(VI) formal oxidation state. The oxidative addition product for W(OH)$_2$(=NH) is five-coordinate, $d^0$ W(OH)$_2$(=NH)(H)(CH$_3$). The geometry of the minimum energy oxidative addition (OA) product is best described as a square pyramid (SQP5) with the imido group in the apical position and singly bonded ligands occupying basal positions. Most structurally characterized[39] L$_4$M=E complexes (M = high-valent metal; L = σ-donor ligand; E = multiply bonded ligand) possess this geometric arrangement, although trigonal bipyramidal (TBP5) W(=NPh)(NMe$_2$)$_4$ exists as a counterexample and a reminder that SQP5 and TBP5 structures can often be quite close in energy.[40] For a TBP5 arrangement with an apical imido there are two isomers depending on whether the hydroxyls are cis or trans. In this case, the cis isomer (**5**) is lower in energy. Following the intrinsic reaction coordinate[20] from the oxidative addition transition state (*vide infra*) to the products leads to the cis isomer which is 10.3 kcal mol$^{-1}$ lower than the trans isomer. This exercise emphasizes the importance of characterizing the vibrational structure of geometries obtained from transition state searches and calculating the IRC to confirm which TS connects which reactants and products.

The W—O bond lengths (1.90 and 1.91 Å) in **5** are similar

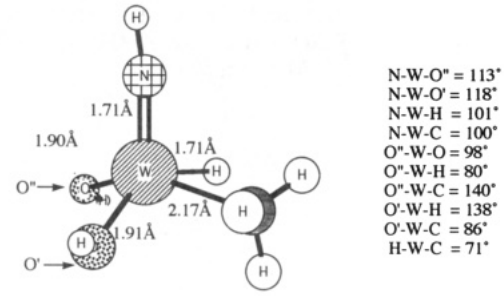


**5**

to those in the reactant (**1a**) and the [2 + 2] product (**2a**). The W—imido bond length (1.71 Å) in **5** is equal to that in W(OH)$_2$(=NH). Qualitative MO arguments for the preference of SQP5 geometries by L$_4$M=E complexes[39] show that a multiply bonded ligand can effectively overlap two perpendicular metal d$\pi$ AOs ($d_{xz}$ and $d_{yz}$ if the W—imido linkage in **5** is taken as the $z$-axis) from the apical position, just as can occur in three-coordinate **1a**; minor diminution of W d$\pi$—N p$\pi$ bonding is thus expected upon going from **1a** to **5**. The W—C bond length in **5** (2.17 Å) is in excellent agreement with average W—C value of 2.19 ± 0.01 Å for square pyramidal W(O)(CH$_2$CMe$_3$)$_3$(NEt$_2$).[33] The complex WH$_6$(PPh(*i*-Pr)$_2$)$_3$ has been characterized by neutron diffraction[41] and the W—H bond lengths measured at 1.728(7) Å, in excellent agreement with the calculated W—H value of 1.71 Å for **5**.

The oxidative addition process is calculated to be exothermic by 9.8 kcal mol$^{-1}$, a difference of ≈33 kcal mol$^{-1}$ from the [2 + 2] pathway, Chart I. The enthalpy for oxidative addition can be estimated from eq 6. Using the

$$\Delta H_{rxn}(\mathrm{OA}) \approx \mathrm{BDE}_{H_3C-H} - \mathrm{BDE}_{W-C} - \mathrm{BDE}_{W-H} \quad (6)$$

mean M—R (R = H, Me) bond energies[36b] for Cp$_2$WR$_2$ (W—H = 74 ± 1 kcal mol$^{-1}$; W—Me = 53 ± 1 kcal mol$^{-1}$) and a methane C—H bond energy of 105 kcal mol$^{-1}$, the estimated $\Delta H_{rxn}$(OA) for the oxidative addition is −22 kcal mol$^{-1}$, in reasonable agreement given the approximations. By calculating the difference between eq 4 and eq 6 it should be possible to estimate the W—N π-bond energy (eq 7). Using the aforementioned values of BDE$_{W-H}$ (∼53

$$\Delta H_{rxn}(\mathrm{OA}) - \Delta H_{rxn}([2+2]) \approx \mathrm{BDE}_{HN-H} - \mathrm{BDE}_{W-H} - \Pi_{MN} \quad (7)$$

kcal mol$^{-1}$) and BDE$_{HN-H}$ (92 kcal mol$^{-1}$) yields a π-bond estimate of 51 kcal mol$^{-1}$. Consideration of the metal—nitrogen bond energy differences[42a] in the gas-phase ions [M(NH)]$^+$ and [M(NH$_2$)]$^+$ (M = Sc, Ti, V) yields estimates of metal—nitrogen π-bond energies ranging from 25 to 35 kcal mol$^{-1}$. The estimate of $\Pi_{WN}$ ≈ 51 kcal mol$^{-1}$ compares with $\Pi_{CN}$ ≈ 63 kcal mol$^{-1}$,[42b] making the calculated value of $\Pi_{WN}$ seem high. The calculations do emphasize the strength of the metal—imido π-bond in these complexes and its potential importance in impeding the progress of methane activation even as a spectator ligand.

**5. Oxidative Addition Transition State.** Oxidative addition is a well-known reaction,[4] having been most thoroughly studied for late, low-valent transition metal

(37) (a) Rabaa, H.; Saillard, J. Y.; Hoffmann, R. *J. Am. Chem. Soc.* **1986**, *108*, 4327. (b) Steigerwald, M. L.; Goddard, W. A. *J. Am. Chem. Soc.* **1984**, *106*, 308. (c) Rappé, A. K. *Organometallics* **1987**, *6*, 354.

(38) $WH_6$ was calculated under the constraint of octahedral symmetry using the same basis sets and ECPs described in Computational Methods.

(39) Nugent, W. A.; Mayer, J. M. *Metal-Ligand Multiple Bonds*; Wiley: New York, 1988.

(40) Berg, D. M.; Sharp, P. R. *Inorg. Chem.* **1987**, *26*, 2959.

(41) Bau, R.; Teller, R. G. *Struct. Bonding* **1981**, *44*, 1.

(42) (a) Clemmer, D. E.; Sunderlin, L. S.; Armentrout, P. B. *J. Am. Chem. Soc.* **1990**, *94*, 3008. (b) Schmidt, M. W.; Truong, P. N.; Gordon, M. S. *J. Am. Chem. Soc.* **1987**, *109*, 5217.

**Chart I. Calculated Reaction Energetics for Methane C—H Activation by $M(OH)_2(=NH)$, M = Ti, W[a]**

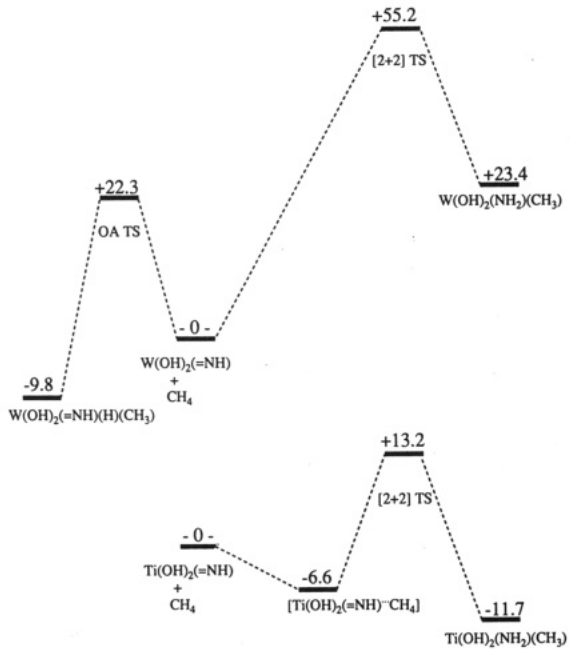


[a] All energies (in kcal mol$^{-1}$) are relative to the reactants (imido plus methane) at infinite separation.

complexes,[21b,c,43] although ion–molecule reactions of alkanes and transition metal atomic ions show oxidative addition to be operant in systems with $d^n$ ($n > 2$).[44] The oxidative addition TS is expected to contain a three-center M···H···C moiety.[4,21b,c,43] Indeed, such a stationary point is found, Figure 2. The single imaginary frequency (1268i cm$^{-1}$) corresponds to C—H bond breaking (C—H bond formation for the microscopic reverse).

The calculated geometry of the oxidative addition transition state is shown in Figure 2 (top) along with the [2 + 2] transition state (bottom of Figure 2) to emphasize their resemblance. Note the remarkable similarity for the triangular W···H···C unit in the two transition states: W—C = 2.32 Å (OA)/2.36 Å ([2 + 2]); C—H = 1.47 Å (OA)/1.47 Å ([2 + 2]); W—H = 1.70 Å (OA)/1.86 Å ([2 + 2]); W—H—C = 94° (OA)/90° ([2 + 2]), Figure 2. Thus, the main difference in the W···H···C moiety is the shorter W···H distance in the oxidative addition versus the [2 + 2] TS, Figure 2. It is possible to use the equations given by Crabtree et al.,[45] eqs 8 and 9 ($r$ = 0.28 Å; 1.30 Å is the

$$d_{bp} = [d_{MH}^2 + r^2 d_{CH}^2 - r(d_{MH}^2 + d_{CH}^2 - d_{MC}^2)]^{1/2} \quad (8)$$

$$r_{bp} = d_{bp} - 1.30\ \text{Å} \quad (9)$$

covalent radius of W, $r_{bp}$ "is effectively the covalent radius of the C—H bonding electrons"), to monitor the progress of the C—H activation events. Inserting the calculated bond lengths from Figure 2 into eqs 8 and 9 yields $r_{bp}$ = 0.47 Å (OA) and 0.59 Å ([2 + 2]), suggesting that the oxidative addition TS is later, relatively speaking, than

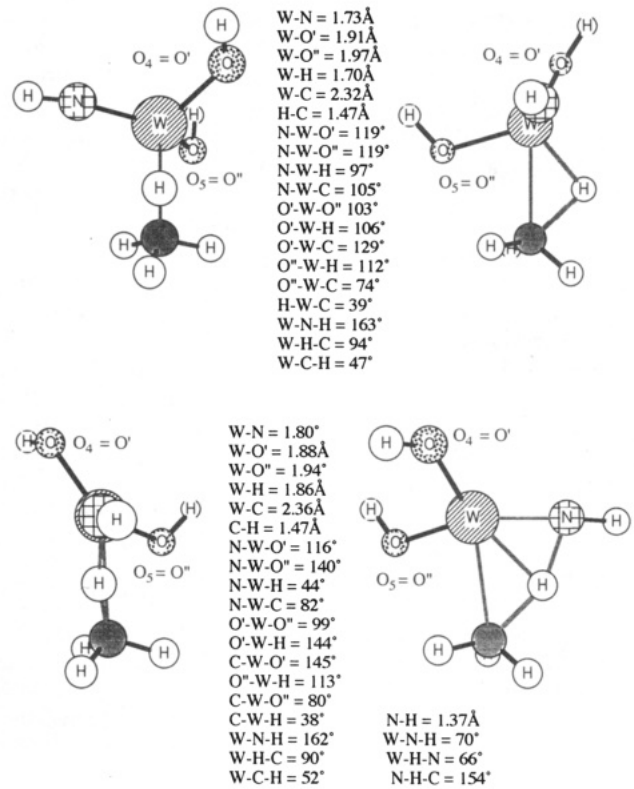


**Figure 2.** Comparison of pertinent metric data for the calculated transition states for oxidative (top) and [2 + 2] (bottom) addition of methane to $W(OH)_2(=NH)$ to form $W(OH)_2(=NH)(H)(CH_3)$ and $W(OH)_2(NH_2)(CH_3)$, respectively. Figures on the right are normal to the W—N—C plane, while those on the left are parallel to the W—N—C plane.

the [2 + 2] transition state, although the numbers are remarkably similar. The major structural change is the position of the OH and NH ligands, Figure 2. While the N is essentially coplanar with the W···H···C moiety (dihedral (H—C—W—N) = +6°) in the [2 + 2] TS, N is roughly perpendicular to W···H···C (dihedral (H—C—W—N) = −84°) in the oxidative addition TS. Inspection of Figure 2 also reveals that the metal—carbon and metal—hydrogen bonds in both transition states are formed to a significant extent, being less than 10% in both cases than metal—carbon and metal—hydrogen bond lengths in the products.

The TS for $W(OH)_2(=NH) + CH_4 \rightarrow W(OH)_2(=NH)(H)(CH_3)$ is 22.3 kcal mol$^{-1}$ above that of the reactants, Chart I. Although the activation barrier for OA is nearly one-half that calculated for the [2 + 2] C—H activation pathway, the barrier is large when compared to "traditional" low-valent C—H activators.[4] Experiments[4c] and calculations[8,21b,43] indicate that C—H oxidative addition to low-valent metals proceeds with very small (≤5 kcal mol$^{-1}$) activation barriers. Wasserman et al.[4c] estimate a barrier of only 5 kcal mol$^{-1}$ for oxidative addition of methane to CpRh(CO). Although, the driving force for $d^8$ $Ir(PH_3)_2(H) + CH_4 \rightarrow Ir(PH_3)_2(H)_2(CH_3)$ is similar to that for $d^2$ $W(OH)_2(=NH) + CH_4 \rightarrow W(OH)_2(=NH)(H)(CH_3)$, −12.8 and −9.8 kcal mol$^{-1}$, respectively, the former reaction has a calculated barrier which is slightly greater than 1 kcal mol$^{-1}$. Thus, the calculations suggest that the low reactivity of these $d^2$ imido complexes is due more to kinetic than thermodynamic considerations.

**6. Intrinsic Reaction Coordinates for [2 + 2] and Oxidative Addition Pathways.** The intrinsic reaction coordinate is defined as the steepest descent path (in mass-

(43) (a) Hoffmann, R.; Saillard, J. Y. *J. Am. Chem. Soc.* **1984**, *106*, 2006. (b) Low, J. J.; Goddard, W. A. *J. Am. Chem. Soc.* **1986**, *108*, 6115. (c) Koga, N.; Morokuma, K. *J. Chem. Phys.* **1990**, *94*, 5454. (d) Ziegler, T. L.; Tschinke, V.; Fan, L.; Becke, A. D. *J. Am. Chem. Soc.* **1989**, *111*, 9177.

(44) Armentrout, P. B.; Beauchamp, J. L. *Acc. Chem. Res.* **1989**, *22*, 315.

(45) Crabtree, R. H.; Holt, E. M.; Lavin, M.; Morehouse, S. M. *Inorg. Chem.* **1985**, *24*, 1986.

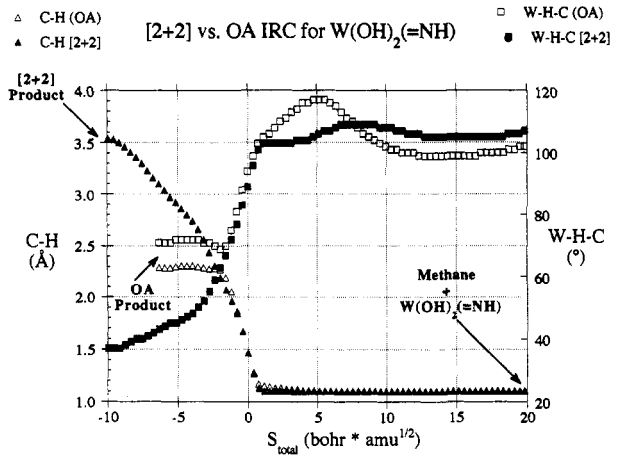


**Figure 3.** C—H distance (triangles) and W—H—C angle (squares) at each calculated IRC point for the C—H bond in methane being activated by $W(OH)_2(=NH)$ by either oxidative (open data points) or [2 + 2] (filled data points) addition.

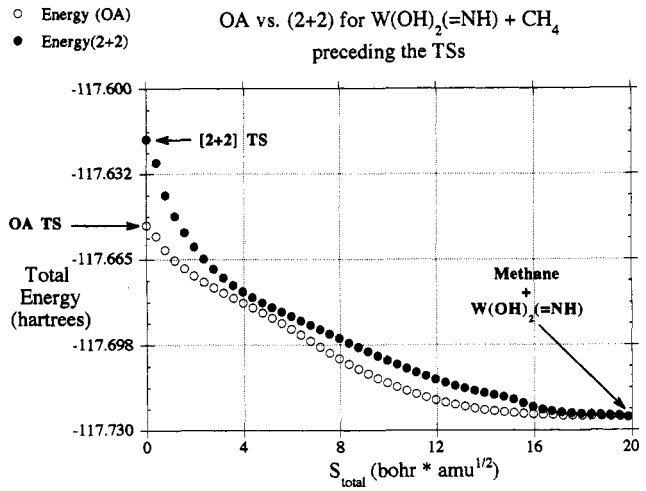


**Figure 4.** Calculated RHF energies for each point along the calculated intrinsic reaction coordinate preceding the transition states for C—H activation of methane by oxidative (open circles) and [2 + 2] (filled circles) addition to $W(OH)_2(=NH)$.

weighted Cartesian coordinates) from TS to the reactants and TS to the products. The IRC can thus be calculated from first principles.[20] Analysis of the IRC yields dynamic information about interactions which control the passage of reactants through the TS and on to the products. In the present case analysis of the IRC can shed some light on the discrimination between the two pathways ([2 + 2] and oxidative addition) since they commence from the same methane plus imido reactants.

In Figure 3 the changes in the C—H distance and M—H—C angle are plotted for the oxidative addition and [2 + 2] intrinsic reaction coordinates. These are the same metric parameters analyzed by Crabtree et al.[45] in their study of C—H oxidative addition. Previous studies[8] of methane activation by C—H oxidative addition to $Ir(PH_3)_2(H)$ show that using either $r_{bp}$ (*vide supra*) or $S_{total}$ (the mass-weighted distance along the reaction coordinate) as the reaction coordinate yields nearly identical curves, so that the latter has been employed. The various TSs are set to $S_{total} = 0$ bohr amu$^{1/2}$). There are two main features in Figure 3 which are worthy of comment.

(i) The C—H bond length remains fairly constant in length as the reaction proceeds from the reactants ($CH_4$ + $W(OH)_2(=NH)$) until undergoing rapid activation at $S_{total} \approx 1.2$ bohr amu$^{1/2}$, Figure 3. Kubas et al.[46] have concluded from analysis of neutron diffraction structures of $\eta^2$-$H_2$ complexes "that the reaction coordinate for H—H bond breaking shows relatively little change in H—H distance until bond rupture is quite imminent, presumably when increased back-bonding can no longer be tolerated". The experimental deductions[46] for the H—H oxidative addition trajectory are consistent with the calculated IRC, Figure 3, for the related C—H oxidative addition. Furthermore, the present calculations suggest that similar dynamic behavior is exhibited by the C—H bond in [2 + 2] C—H activation. The calculated charge on the methane fragment along the oxidative addition IRC for the $d^2$ W—imido shows the same behavior that was seen in the OA intrinsic reaction coordinate for $Ir(PH_3)_2(H) + CH_4 \rightarrow Ir(PH_3)_2(H)_2(CH_3)$; i.e. the charge on the methane increases until the C—H "break point" at $S_{total} \approx 1.2$ bohr amu$^{1/2}$ and then becomes less positive as the reaction proceeds, Figure 3. We have interpreted this in terms of a two-step process:[8] substrate-to-complex donation is needed to get the reactants into the vicinity of the transition state (electrophilic phase), but eventually complex-to-substrate back-donation (nucleophilic phase) must occur to cleave the C—H bond.

(ii) Despite the great difference in the ultimate fate of the C—H bond, the rough shapes of the C—H and M—H—C curves are quite similar for both [2+2] and oxidative addition, particularly in the portion of the reaction preceding the transition state. This similarity was noted in the comparison of C—H oxidative addition to a $d^8$ Ir complex and [2 + 2] addition of C—H to the W—imido bond in a $d^0$ W complex.[8] It is now that the advantage of comparing [2 + 2] and oxidative addition for the same complex becomes apparent. As the reactants are the same, the starting energies will, of course, be equal for both reactions. In Figure 4 the RHF energies are plotted for points along the IRC from the reactants to the transition state. One can envision methane approaching $W(OH)_2(=NH)$ and proceeding down either the [2 + 2] or oxidative addition reaction channel. The geometric similarity of the [2 + 2] and oxidative addition transition states (*vide supra*) suggests that interconversion between the two reaction channels may be relatively facile. Perhaps the most significant detail revealed by comparison of the OA and [2 + 2] IRCs, Figures 3 and 4, for $W(OH)_2(=NH)$ + $CH_4$ is the relatively late point at which discrimination between the two pathways occurs. It is not until the reactions have each proceeded fairly close to the transition state ($S_{total} \approx 2.0$ bohr amu$^{1/2}$) that significant differences (>10 mhartrees) in energy are realized, Figure 4.

## Summary and Conclusion

The activation of methane by the $d^2$ imido complex, $W(OH)_2(=NH)$, has been studied using effective core potential methods. Methane activation by oxidative addition (to yield a five-coordinate, $d^0$ hydrido(methyl) product) and [2 + 2] C—H addition to the metal—imido linkage (to yield a $d^2$ amido(methyl) product) were investigated. The [2 + 2] C—H activation pathway was compared with the related $d^0$ $Ti(OH)_2(=NH)$, a model of a putative methane activating transient.[11b] Several points have emerged from this study and are summarized below.

(46) Kubas, G. J.; Burns, C. J.; Eckert, J.; Johnson, S. W.; Larson, A. C.; Vergamini, P. J.; Unkefer, C. J.; Khalsa, G. R. K.; Jackson, S. A.; Eisenstein, O. *J. Am. Chem. Soc.* **1993**, *115*, 569.

(1) Calculations show both the $d^0$ Ti— and $d^2$ W—imido complexes to have a high positive charge on the metal and a significant degree of metal—imido polarization. The essential difference between these two is the occupancy of a metal-based frontier MO—the HOMO for the $d^2$ complex and the LUMO for the $d^0$ complex. As the methane–complex interaction has a substantial covalent contribution[7b] to the bonding, the absence of the metal-based LUMO means that $W(OH)_2(=NH)$ cannot coordinate weak Lewis bases such as methane.

(2) The [2 + 2] addition of a methane C—H bond across the imido linkage is exothermic for $Ti(OH)_2(=NH)$, by 11.7 kcal $mol^{-1}$, and endothermic for $W(OH)_2(=NH)$, $\Delta H_{rxn} = +23.4$ kcal $mol^{-1}$, in agreement with the difference in reactivity of $d^0$ Ti— and $d^2$ W—imidos.

(3) The enthalpy of activation ($\Delta H^{\ddagger}_{act}$) for the [2 + 2] mechanism is 55.2 kcal $mol^{-1}$ for $W(OH)_2(=NH)$ and 13.2 kcal $mol^{-1}$ for $Ti(OH)_2(=NH)$, versus separated reactants. The calculated enthalpy of activation for the Ti reaction is near that for the only $\Delta H^{\ddagger}_{act}$ measured for C—H activation by a multiply bonded $d^0$ complex.[3a]

(4) Oxidative addition of a methane C—H bond to $W(OH)_2(=NH)$ has a much larger thermodynamic driving force than the [2 + 2] process. The oxidative addition process is calculated to be exothermic by 9.8 kcal $mol^{-1}$. Additionally, the TS for OA is 22.3 kcal $mol^{-1}$ above the reactants, much less than found for the [2 + 2] pathway. However, the barrier is much larger than OA barriers for traditional low-valent C—H activators,[4] despite comparable thermodynamic driving forces,[8] suggesting a kinetic origin for the inertness of the $d^2$ imidos.

(5) The TSs for the [2 + 2] and oxidative addition reactions are similar in geometry, particularly for the W···H···C active site. The major structural change between the two TSs lies in the relative positions of the OH and NH ligands. The oxidative addition TS occurs later along its reaction coordinate than does the [2 + 2] TS. The C—H bond length remains constant along the oxidative addition trajectory, until the TS is imminent, supporting deductions about H—H oxidative addition made from analyses of classical and nonclassical polyhydrides.[4b] The calculations suggest that similar behavior is exhibited by the [2 + 2] C—H activation trajectory.

(6) The shapes of the C—H and W—H—C curves (Figures 3 and 4) are similar for both [2 + 2] and oxidative addition in the portion of the reaction preceding the TS. Discrimination between the pathways, in an energetic sense, does not occur until the reactions have proceeded well into to the neighborhood of TS.

Given that the increase in C—H bond length, the decrease in W—H—C angle, and the changes in electron density on the methane fragment occur in the same region of the IRC ($S_{total} \approx 1$–2 bohr $amu^{1/2}$), it is not unreasonable to infer a connection between events. The reactants approach the point at which the reaction turns over from the electrophilic to nucleophilic phase and then the substrate must "choose" the most readily available source of electrons in the complex to populate $\sigma^*_{CH}$ and permit C—H scission. For $d^2$ $W(OH)_2(=NH)$ this source is clearly the metal-based HOMO and thus the reaction proceeds onto oxidative addition. Alternatively, if the potential surface connecting the two pathways is not soft, the reactants may proceed down the [2 + 2] path and then back out (perhaps many times) until the more favorable oxidative addition pathway is sampled.

A methane adduct would seem to be an ideal vehicle to allow for multiple samplings of reaction channels until the most favorable one is located. It is clear that the formation of an adduct is a convenient means of getting the reactants closer to the TS with less energetic investment. While $W(OH)_2(=NH)$ and methane show significant substrate–complex repulsion at $S_{total} > 10$ bohr $amu^{1/2}$ (metal—carbon separations of >3.4 Å), the $Ti(OH)_2(=NH)\cdots CH_4$ adduct is an accessible point preceding the TS ($S_{total} = 0$ bohr $amu^{1/2}$) at $S_{total} \approx 7$ bohr $amu^{1/2}$ (Ti—C = 2.84 Å).[7b] What is less clear is whether or not the molecular and electronic structure of the adduct plays any role in facilitating the important C—H scission step which follows. It is interesting that, in the present case, we have a complex which does not form an adduct (i.e., $d^2$ $W(OH)_2(=NH)$) and has a much higher barrier to C—H oxidative addition than a "traditional" low-valent system (i.e., $d^8$ $Ir(PH_3)_2(H)$) which can form a stable adduct, despite similar thermodynamic driving forces for each. It is also conceivable that an adduct may serve to orient the reactants for the C—H activation event, increasing the rate by increasing the preexponential factor in the Arrhenius equation. It has been postulated for electrophilic $Pt^{II}$ and $Hg^{II}$ systems that methane adducts are formed.[5c,d] As seen above, it is not sufficient that the metal be electrophilic in an electrostatic sense but that it have the necessary low-energy unoccupied MOs to form an adduct. These calculations provide some of the first computational clues as to the possible importance of methane adducts in C—H activation. In order to evaluate their role more fully studies are underway in our labs to evaluate $d^n$ ($n \geq 4$) systems which are capable of C—H activation by both oxidative addition and [2+2] pathways and for which a methane adduct is formed prior to C—H scission.

**Acknowledgment.** The National Science Foundation (through its support of the National Center for Supercomputing Applications, Grant No. CHE920027N), the Joint Institute for Computational Science at the University of Tennessee—Knoxville (for providing access to the iPSC/860 and CM-5 parallel supercomputers at Oak Ridge National Laboratory and UTK, respectively), IBM (participation in the Developer's Discount Program), the Air Force Office of Scientific Research (Grant 93-10105), and the donors of the Petroleum Research Fund, administered by the American Chemical Society, are gratefully acknowledged for their support of computational transition metal chemistry at Memphis State.

OM930299C